Investigation of the neuroprotective effects of squid ink extract to mitigate the reactive oxidative species in stress-induced neuroblastoma cell line

Elangovan Sujatha and Arumugam Sivakumar*
Protein Engineering Laboratory, School of Biosciences and Technology, Vellore Institute of Technology, Vellore, Tamil Nadu, INDIA
*siva_kumar.a@vit.ac.in

Abstract

Neurodegeneration due to exposure to oxidants has severe effects on neuronal loss when exposed for a prolonged period, causing them to loss neurons. The degeneration of neurons in the substantia nigra decreases the production of dopamine in the brain, which can further act as an initiator for the early onset of Parkinson's disease (PD). Carbidopa-levodopa is the standard drug used in the treatment of PD, but it comes with a drawback of drug side effects in the long run. Marine compounds exhibit potential for drug discovery and are rising to overcome these shortcomings in the existing drugs. We assessed and optimised the half maximum inhibitory concentration (IC_{50}) of stress-induced models for hydrogen peroxide and acrylamide, as well as the standard drug levodopa (LD) and squid ink (SI) extract using 3-(4,5-dimethylthiazol-2-yl)-2,5-diphenyltetrazolium bromide (MTT) assay and evaluated their cytotoxic effects. Reactive oxygen species (ROS), cell apoptosis, colony formation, DNA fragmentation, cell migration and gene expression studies were evaluated through 2',7'-dichlorofluorescein diacetate (DCFH-DA), flow cytometry, proliferation assay, 4',6-diamidino-2-phenylindole (DAPI), scratch test assay and real-time quantitative polymerase chain reaction (RT-qPCR) respectively.

The cell viability assay exhibited IC_{50} values of 77±0.14, 79±0.17 and 82±0.21 µg/ml concentrations for control, hydrogen peroxide and acrylamide groups respectively. The ROS assay showed significant antioxidant activity in the stress-induced groups compared to the LD-treated group. Likewise, DAPI staining showed lesser DNA fragmentation in stress-induced cells in SI-treated groups. Similarly, the flow cytometry exhibited increased cell viability in SI-treated stress-induced cells. The gene expression studies in SI-treated revealed the downregulation of pro-apoptotic genes. SI-extract exhibited potential antioxidant properties. Further, we recommend performing extensive screening of these marine compounds to obtain potential therapeutics to overcome neurodegenerative diseases caused due to oxidative stress.

Keywords: Squid ink extract, oxidative stress, neurodegeneration, antioxidant, apoptosis, cell viability.

Introduction

Neuroblastoma (NB) cell lines are human-derived, subcloned three times from the SK-N-SH[1], which is derived from a 4-year-old patient through bone marrow biopsy to obtain SH-SY5Y cell lines[2]. These SH-SY5Y cell lines are of great importance and serve as a tool for *in vitro* studies due to their ability to mimic dopaminergic neurons[3], which make them a tool to study neurodegeneration of brain cells such as Alzheimer's disease[4], Parkinson's disease[5], ischemia[6], amyotrophic lateral sclerosis[7] as well as neurotoxicity[8] and neurorestoration[9]. SH-SY5Y cell lines were first subcloned in 1978 and it has undergone a large number of passages up to this date and due to this which they are considered to have phenotypic stability and are defined as 'neuron-like' structures with further induction to differentiation from their undifferentiated state.

Since these NB cells express opioids[10], nerve growth factor (NGF)[36] and muscarinic receptors[47], they act as an excellent tool for research on dopaminergic systems. Even though the undifferentiated NB cells have restrictions in expression of particular pathways or studies, they are widely used to study apoptosis, reactive oxygen species (ROS), gene expression and molecular studies, immunofluorescence assay, cell migration and proliferation studies for neurodegenerative diseases[13-17].

Hydrogen peroxide is a powerful oxidant that damages healthy cells naturally by producing free radicals which lead to suppression of dopamine in the substantia nigra, leading the neuronal loss or neurodegeneration through apoptosis or, in some cases, necrosis. Exposure to oxidants including hydrogen peroxide[44], acrylamide[7], menadione[58], sodium nitroprusside[33] and paraquat[34], can cause early onset of neurodegeneration, which leads to Parkinson's disease (PD) at a later stage. Neurotoxins which induce PD, such as 1-methyl-4-phenyl-1,2,3,6-tetrahydropyridine (MPTP)[67], rotenone[4.31], 6-hydroxydopamine (6-OHDA)[2] and lipopolysaccharide (LPS)[62], mimic different aspects such as mitochondrial dysfunction, neuroinflammation, oxidative stress and aggregation of α-synuclein forming Lewy bodies[27-30].

Neurodegerative disease is mainly caused due to the oxidative stress which further leads aging of brain cells[25]. With rising concerns of its complexity of neurodegenerative

diseases treatment with shakiness, involuntary muscle movement, brain fog and hallucinations to the levodopa-carbidopa drug treatment in Parkinsons's disease, natural and marine sources for potential drug discovery rich in antioxidants[24] have become significant to overcome the shortcomings of prolonged exposure to the drug[1]. Carbidopa belongs to the group of medicines called aromatic L-amino acid decarboxylase inhibitors (AADC)[43], combined with levodopa to assist in reaching the blood-brain barrier (BBB)[23] without breaking down into dopamine in the blood and gut before reaching the brain.

Based on this, an *in vitro* study was hypothesized to evaluate the neuroprotective effects of squid ink extract, a marine source, against stress-induced neuroblastoma cell models by conducting a series of studies and examining their wound healing effects to obtain new drug discovery for the treatment of oxidative stress-related neurodegenerative diseases.

Material and Methods

Cell culture and reagents: SH-SY5Y neuroblastoma (NB) cells were purchased from NCCS, India. The NB cell line was cultured in Ham's F-12 medium (Gibco) supplemented in Fetal Bovine Serum (FBS) (HiMedia) and 1% antimycotic solution (HiMedia). The cells were incubated in 37°C at 5% CO_2 incubator. Trypsin-EDTA (Gibco), MTT (Sigma), DAPI (Sigma) and DCFH-DA (Sigma) were purchased. Levodopa was purchased from Sigma.

Sample collection and preparation: The *Uroteuthis duvaucelli,* also known as the Indian squid, was freshly collected from Kasimedu fish harbour, Chennai, Tamil Nadu, India and transported safely to the lab in chilled conditions. The ink from the squid ink was prepared with a slight modification[14]. The non-melanin layer of the ink was removed by washing the ink with distilled water at 20,000 rpm for 15 mins at 4°C. Hexane was added to the pellet and centrifuged at 10,000 rpm for 25 mins at 4°C. The pellet was lyophilized and the moisture-free powder sample was homogenized into fine powder. Further, the powdered sample was added to 1x phosphate buffer saline (PBS) and sonicated to dissolve the sample. The sample was filtered using Whatmann filter paper and stored in light-sensitive tubes for further studies.

Characterisation of squid ink extract

Morphological characterization through Transmission Electron Microscopy: The freeze-dried ink powder was further analysed to study the morphological characterisation through transmission electron microscopy[19] (TEM) through FEI – TECNAI G2-20 TWIN (Operating voltage 200 kV).

High Performance Liquid Chromatography (HPLC): High-performance liquid chromatography (HPLC) was performed in Agilent Infinity 2000 equipped with a C18 HPLC column. The flow range was maintained at 0.1 ml/min and the column temperature was kept at 20 to 25°C. Samples were filtered through a 0.22 µm syringe filter before sample injection[11]. The mobile phase consisted of solvent A: water with 0.1% formic acid and solvent B: acetonitrile.

Maintaining SH-SY5Y cell lines: The SH-SY5Y cells were cultured in Ham's F-12 medium with FBS and 1% antimycotic solution, maintained under optimum conditions at 37°C and 5% CO_2 incubator. The cells were passaged at 80-85% confluency[56].

Stress induction in SH-SY5Y cell lines: Cells were stress induced using hydrogen peroxide[41] and acrylamide[73] using ten different varying concentrations of 50-500 µM and 0.1-1.0 mM respectively for 24 hrs prior drug treatment.

Cell viability assay: $1x10^5$ cells were seeded in a 96-well plate and incubated for 24 hrs, followed by stress induction using hydrogen peroxide (50-500 µM) and acrylamide (0.1-1.0 mM). Varying concentrations of squid ink extracts (10 to 100 µg/ml) were mixed along with the medium and incubated for 24 hours. Finally, 0.5 mg/ml MTT solution was added to each well and incubated at 37°C for 4 hours under dark conditions[55]. Formazan crystals were dissolved by adding 150 µl DMSO per well and absorbance was measured using a microplate reader at 570nm.

Reactive oxygen species (ROS) analysis: The intracellular ROS of the cells was determined using the DCFH-DA staining method. $1x10^5$ cells were seeded in 35x10mm cell culture dishes with complete Ham's F-12 medium[57]. DCFH-DA was dissolved in FBS-free medium to a final concentration of 10µM. Cells were incubated for 30 min at 37°C under dark conditions and washed three times with serum-free medium. Fluorescence was measured at a wavelength of 480/530 under a fluorescence microscope with an imaging system (WESWOX FM-3000, India).

DNA fragmentation assay: Nuclear morphology of SH-SY5Y cells pre- and post- H_2O_2 and acrylamide exposure was analysed using 4',6-diamidino-2-phenylindole dihydrochloride (DAPI) staining. $1x10^5$ cells were seeded in culture dishes and were fixed with 4% paraformaldehyde (PFA) for 20 minutes at room temperature. Further, the cells were washed and permeabilized using 0.25% Triton X-100 in 1x PBS for 10 minutes. Staining was performed using 100µM DAPI for 15 minutes at room temperature. Samples were rinsed gently with distilled water and 10µl of 1x PBS was added to the dish before visualization under the microscope (WESWOX FM-3000)[32].

Flow cytometry analysis: Cell apoptosis was performed using the Annexin V-FITC kit (Elabscience), according to the instructions in the manufacturer's protocol. Following cell seeding and drug treatment, $1x10^5$ cells were pelleted by centrifugation and subsequently resuspended in 250 µL of Annexin V binding buffer. 5 µL of Annexin V-FITC and 10 µL of propidium iodide (PI) conjugate solution were added to the suspension. The samples were vortexed gently and

incubated at 37°C for 15 minutes under dark conditions[52]. Finally, apoptotic cell populations were quantified with flow cytometric analysis using fluorescence-activated cell sorting (FACS) (CytoFLEX, Beckman Coulter, USA).

Colony forming assay: Cells were cultured under standard conditions for 21 days, during which colony formation was assessed. Following the incubation period, colonies were fixed in fixing solution methanol: acetic acid (3:1) and stained using a 0.1% (w/v) crystal violet solution prepared in 3.5% formaldehyde at room temperature, after an initial wash with tap water[17].

Cell migration assay: The cell migration was assessed by creating a monolayer wound in SH-SY5Y cells without FBS with a cell density of $1x10^5$ cells per dish. A linear wound was created using a 10 µL sterile pipette tip at 80% confluency[54]. The culture medium was replaced with SI-extract-medium with varying concentrations (10 to 100 µg/ml) prepared in 1x PBS. Cell migration was monitored at 0,12 and 24 hours using an inverted microscope (Labomed TCM-400, USA). Wound closure was quantified by measuring the gap distance at two independent wound sites per experimental group.

Quantitative real-time PCR (qRT-PCR): SI-extracts were added at their IC_{50} concentration for a period of 24 hours. The RNA was isolated using the TRIzol reagent according to the manufacturer's protocol (Takara). RNA quantification was done at 260nm and the synthesis of the cDNA strand was performed according to the manufacturer's protocol using PrimeScript RT reagent kit (Takara). The gene expression studies were performed in the CFX96 Touch Real-Time PCR Detection System, Biorad, according to the manufacturer's protocol using the TB Green® Advantage® qPCR Premix (Takara)[5].

β-tubulin III was used as the internal control gene. The forward and reverse primer sequences of all the genes are shown in table 1. qRT-PCR gene expression was analysed using the $2^{-\Delta\Delta Ct}$ method and normalised to the β-tubulin III gene.

Statistical analysis: All experiments were conducted in triplicate and represented in mean ± standard deviation (SD). Statistical analysis was performed using GraphPad Prism 8.0.1. For comparison between multiple groups, an ordinary one-way ANOVA followed by Dunnett's multiple comparison test was applied. A p-value of $p < 0.05$ was considered statistically significant where * indicates $p < 0.05$, ** indicates $p < 0.01$, *** indicates $p < 0.005$ and **** indicates $p < 0.001$.

Results

Morphological difference in stress-induced cells: The SH-SY5Y cells showed a significant change in their shape compared to the healthy cells. The morphology of normal cells exhibits a spindle, elongated structure whereas in the cells under stress, induced by hydrogen peroxide and acrylamide, the nucleus of the cells has a shrunken nucleus with spherical cell structure as shown in figure 1.

TEM showing the morphological characterization of SI-extract: In figure 2, the SI-extract exhibits loose aggregates, monodisperse with uniformity and shows spherical nanoparticles with narrow size distribution as well as partial aggregation. At 200nm they have well-defined spherical particles where the surfaces appear smooth, but the core is denser than the outer layer. From the analysis, the radius of the outer shell was 171.15 nm, whereas the inner core was 91.24 nm in size.

Characterization of squid ink extract using *HPLC*: Qualitative HPLC performed for the SI-extract exhibits peaks at various time ranges at 5.058, 6.196, 6.499, 7.601 and 8.785 minutes. At 5.058 minutes, the peak indicates a high abundance of smaller polar metabolites which can represent the presence of L-DOPA, aromatic amino acids, or taurine. The peaks at 6.196 and 6.499 minutes show an overlapping short peak, as shown in figure 3, which show the possible presence of small phenolic compounds and small peptides and at 7.601 minutes, the peak shows the presence of polar pigment or a peptide. Melanin is a large pigment that elutes finally at 8.785 minutes, which is represented by a broad peak.

Cell Viability Assay: The SH-SY5Y cells were treated with varying concentrations of hydrogen peroxide for 24 hrs and the optimal stress induction was 400 µM of hydrogen peroxide and 1mM of acrylamide, which was further used for cytotoxicity stress inducing model[65]. The stress-induced cells by 400µM of H_2O_2 and 1mM of acrylamide, reduced the viability of neuroblastoma cells to 43.9±1.8% in comparison to control cells. The control and stress-induced cells were treated with differing concentrations of SI extracts (10 to 100 µg/ml) protecting the cells against oxidative stress. The survival of SH-SY5Y cells was improved with increasing drug concentration, but specifically at 77±0.14, 79±0.17 and 82±0.21 µg/ml concentration for control, hydrogen peroxide and acrylamide induced groups respectively as shown in figure 4.

Stress-induced squid ink extract-treated cells mitigating reactive oxygen species (ROS): DCFH-DA assay evaluated the antioxidant potential of squid ink with levodopa as the standard drug in SH-SY5Y neuroblastoma cells. Cells treated with squid ink extracts showed significantly lower fluorescence intensity compared to those treated with levodopa which indicates effective reduction of ROS accumulation as shown in figure 5.

The ROS generation of SI-treated cells in control, hydrogen peroxide and acrylamide was 38%, 26% and 22% whereas in the LD-treated groups, it was 57%, 43% and 38% and for no drug treatment group, it was 79%, 83% and 89% respectively.

Table 1
List of genes and primer sequences used for the study.

Role	Gene	Forward primer (5'-3')	Reverse primer (3'-5')
Pro-apoptotic	BAX	GCCCTTTTGCTTCAGGGTTTC	GCAGGGTAGATGAATCGGGG
	CASP3	CATGGAAGCGAATCAATGGACT	CTGTACCAGACCGAGATGTCA
Anti-apoptotic	BCL-2	GAACTGGGGGAGGATTGTGG	CATCCCAGCCTCCGTTATCC
	BCL-XL	CGGATTTGAATCTCTTTCTCTCCC	CGACCCCAGTTTACCCCATC
Antioxidant	SOD1	GGTGGGCCAAAGGATGAAGAG	CCACAAGCCAAACGACTTCC
	CAT	CTCCGCCGAGTCAGAGTTG	CCTTTGCCTTGGAGTATTTGGTA
	GPX1	CAGTCGGTGTATGCCTTCTCG	GAGGGACGCCACATTCTCG
Internal control gene	β-tubulin III	TCTCACAAGTACGTGCCTCG	CTCCGTGTAGTGACCCTTGG

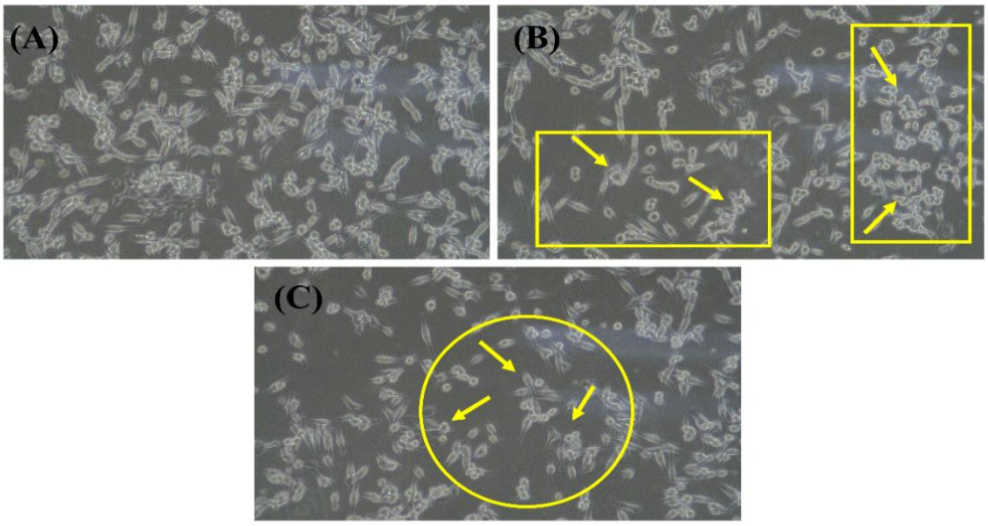

Figure 1: Microscopic imaging shows morphological differences in (A) normal cells without stress showing undifferentiated spindle shape, (B) cells treated with 400mM of hydrogen peroxide and (C) cells treated with 1mM of acrylamide, where the cells under stress partially lose spindle shape.

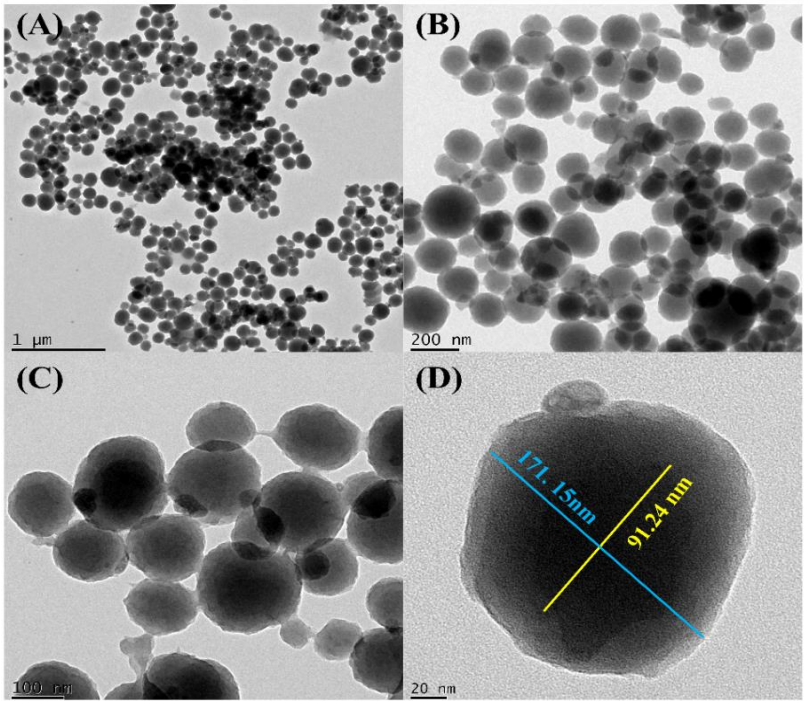

Figure 2: Morphological characterisation of lyophilized squid ink (A) 1 µm, (B) 200 nm, (C) 100 nm and (D) 20 nm.

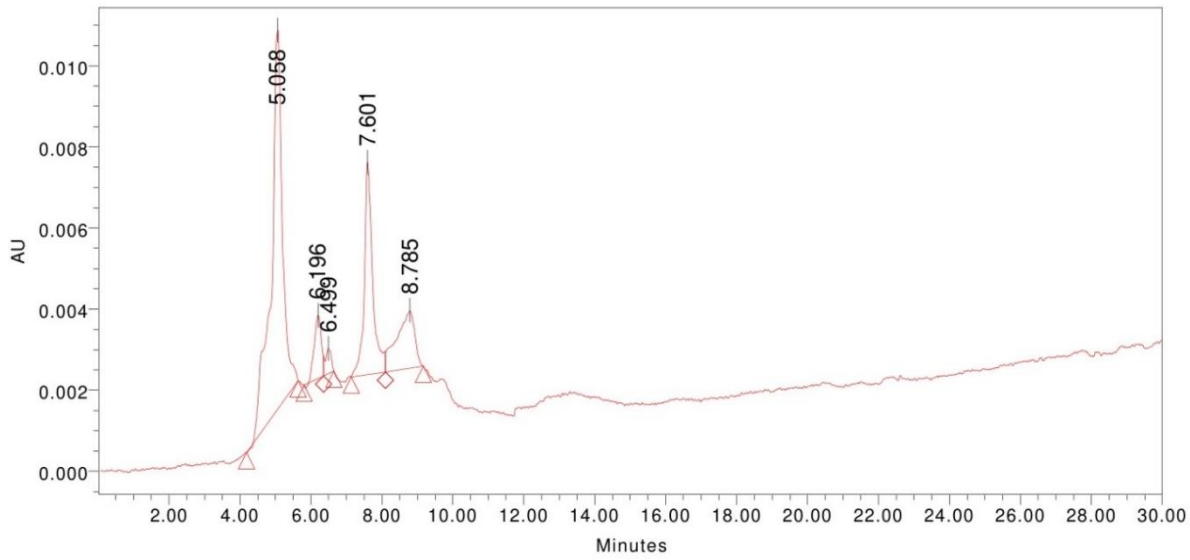

Figure 3: HPLC chromatogram of squid ink extract with acetonitrile as mobile phase

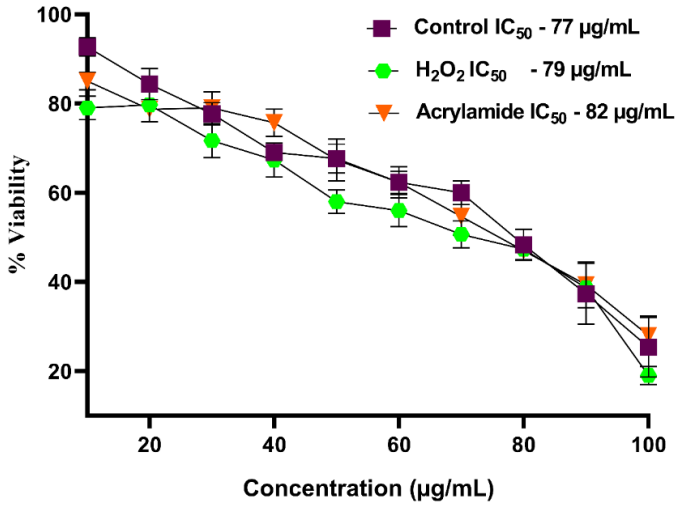

Figure 4: Cytotoxicity assay showing cell viability of control and stress-induced SH-SY5Y cells by MTT assay.

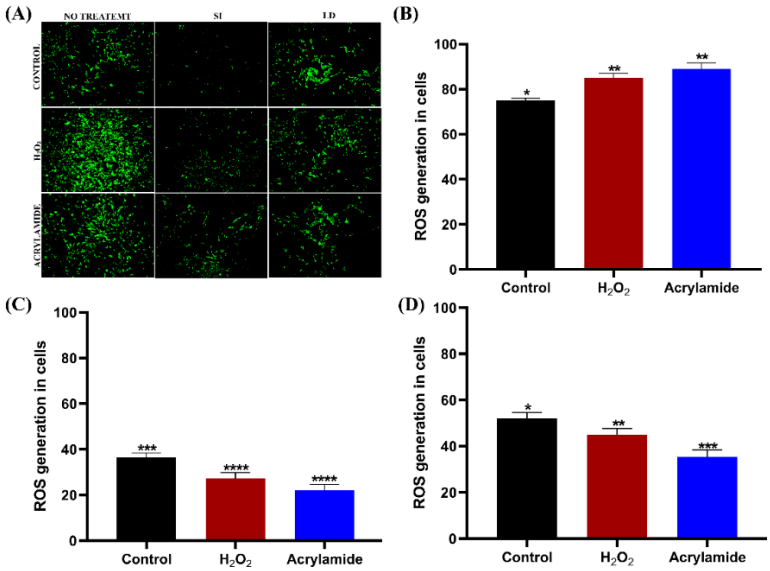

Figure 5: Reactive oxygen species assay using DCFH-DA stain illustrating the antioxidant potential against squid Ink (SI) with standard levodopa (LD) categorized into control, hydrogen peroxide and acrylamide-induced neuroblastoma cell lines where (A) ROS activity under phase contrast fluorescent microscope, (B) without drug treatment, (C) SI extract treated and (D) LD treated groups.

SI extract protects neuroblastoma cells from apoptotic cell death: The ability to induce apoptosis in drug-treated cells was evaluated using flow cytometry. In SH-SY5Y cell lines, viable cells were evaluated to be 88.82% (SI+control), 50.97% (SI+H_2O_2) and 85.56% (SI+acrylamide) as shown in figure 6. Similarly, in the LD-treated cells, the cell viability was evaluated as 47.62% (LD+control), 40.83 (LD+ H_2O_2) and 42.26 (LD+acrylamide) and the cells with no drug treated showed only 16.46% of viable cells.

Colony forming assay exhibits proliferative effects on SI-treated neuroblastoma cells: The SI extract pre-treated groups showed increased proliferation compared to the control and standard groups. In addition to this, the SI extract pre-treated control group and stress-induced hydrogen peroxide and acrylamide group showed a proliferation of 78.85%, 76.75% and 82.15% respectively. The levodopa-treated control, hydrogen peroxide and acrylamide group exhibited 59.45%, 57.65% and 54.34% respectively as shown in figure 7. The cell survival rate was negligible in the non-treated groups comparatively.

Nuclear fragmentation assessment exhibiting an intact cellular nucleus: The cells pre-treated with squid ink extract at its IC_{50} value before inducing stress exhibited reduced apoptosis, as shown in figure 8. Quantitative analysis confirmed a reduction in apoptotic nuclear features from 33.5% (control), 74.66 % (H_2O_2) and 98.33% (acrylamide) to 17.5% (SI extract + control), 56.45 % (SI extract + hydrogen peroxide), 53.33% (SI extract + acrylamide), 24.45% (LD + control), 69.95% (LD + hydrogen peroxide) and 81.23% (LD + acrylamide) respectively.

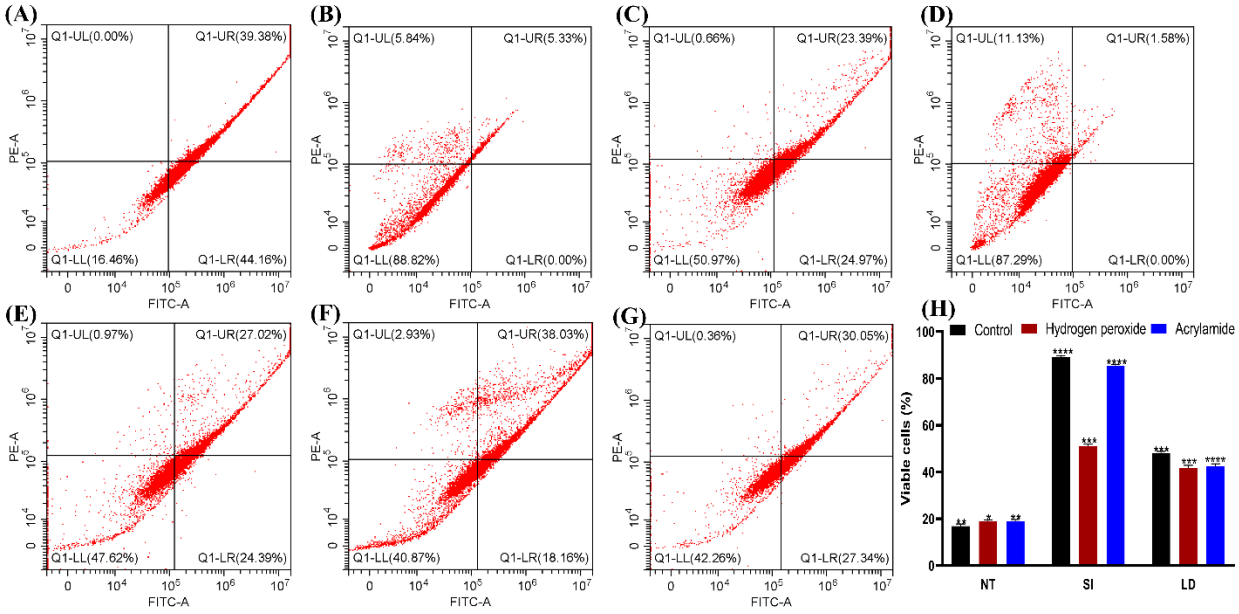

Figure 6: Flow cytometry analysis showing a decreased cell viability in (A) untreated group, with a significant increase in cell viability in SI-treated groups (B-control, C-hydrogen peroxide and D-acrylamide) compared to the levodopa-treated groups (E- control, F-hydrogen peroxide and G- acrylamide) and (H) exhibits the cell viability (%) in all groups [NT-no treatment, SI-squid ink and LD-levodopa].

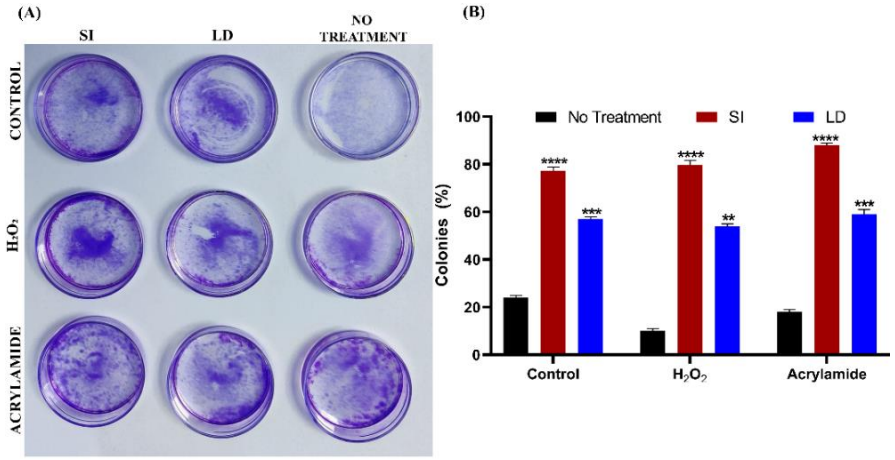

Figure 7: Colony formation assay showing (A) the colonies formed in control, hydrogen peroxide and acrylamide groups against squid ink (SI) and levodopa (LD) treated groups and (B) % of colonies formed in the proliferation assay.

Cell migration assay demonstrating wound healing properties of SI-extract: The wound repair of neuroblastoma cells was performed using squid ink extract with levodopa as the standard drug in SH-SY5Y cells. The control group without any treatment exhibited minimal cell migration.

On the contrary, cells pre-treated with squid ink extract under oxidative stress conditions and normal conditions showed significant cell migration, with substantial gap closure within 24 hours. Both the stress-induced (control, H_2O_2 and acrylamide) groups pre-treated with squid ink exhibited accelerated cell migration compared to the untreated groups as shown in figure 9.

qRT-PCR revealing downregulation of pro-apoptotic genes preventing apoptosis: The level of mRNA expression fold change was analysed by the $2^{-\Delta\Delta Ct}$ method and normalised to β-tubulin III internal control gene. The treatment with squid ink extract potentially regulated the genes compared to that of the standard drug.

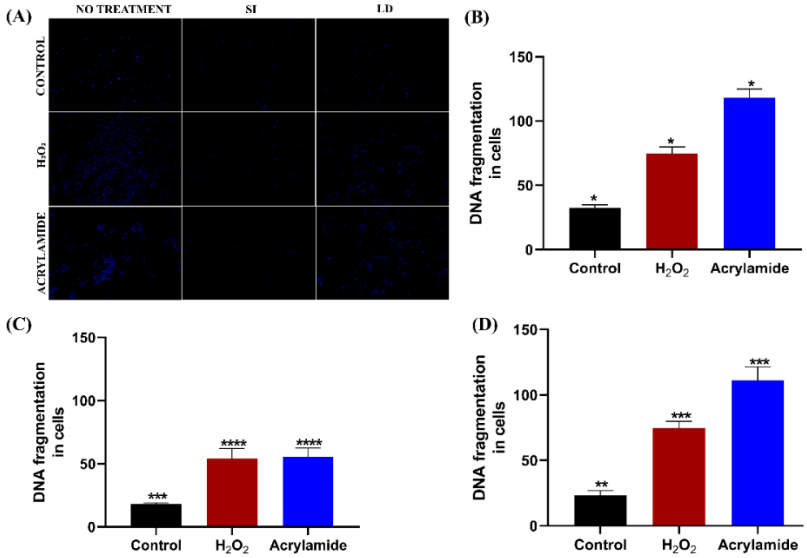

Figure 8: DAPI staining shows (A) nuclear fragmentation against (B) no drug treatment group, (C) SI-treated and (D) LD-treated, categorized into control, hydrogen peroxide and acrylamide-induced SH-SY5Y cells.

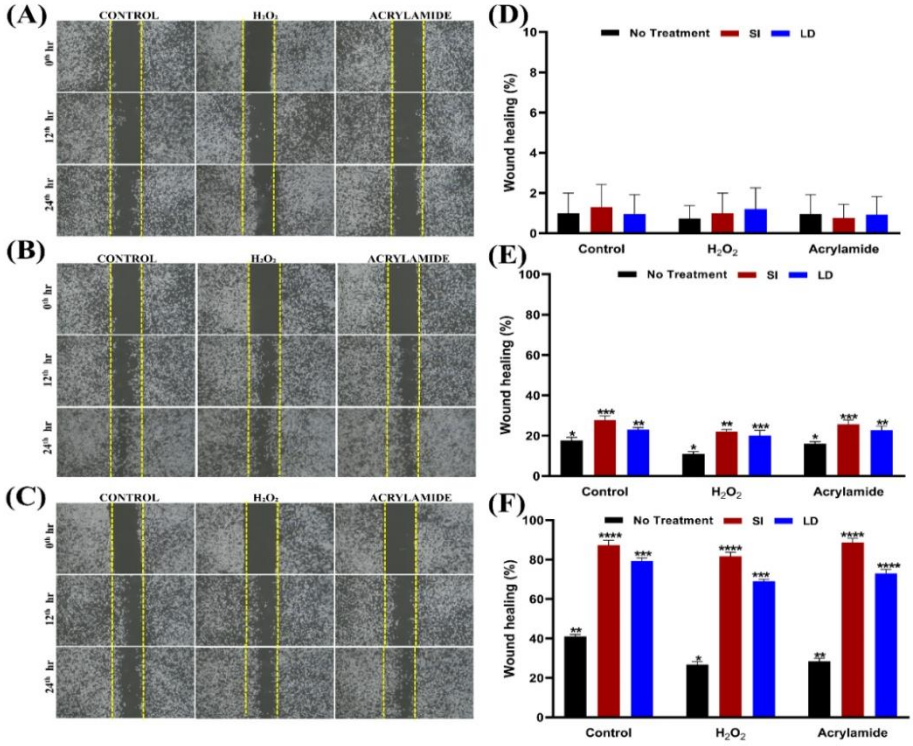

Figure 9: Cell migration assay exhibits (A) no drug treatment, (B) SI extract treated, (C) levodopa (LD) categorized into control, hydrogen peroxide and acrylamide-induced neuroblastoma cell lines in a time-dependent manner, the percentage of wound healing at (D) 0th hour, (E) 12th hour and (F) 24th hour.

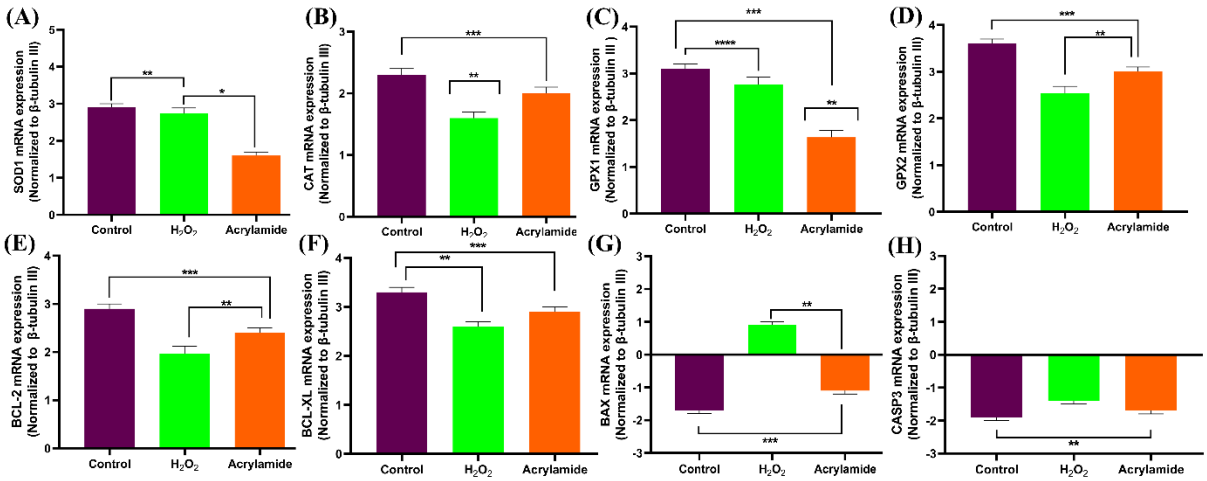

Figure 10: The gene expression with SI-treated exhibits the upregulation of antioxidant genes SOD1, CAT, GPX1 and GPX2 (A-D) and anti-apoptotic genes BCL-2 and BCL-XL (E and F) and downregulation of pro-apoptotic genes BAX and CASP3 (G and H).

In SH-SY5Y stress-induced cells, the treatment with squid ink extract upregulated the anti-apoptotic (BCL-2, BCL-XL) and antioxidant-related genes (SOD1, CAT and GPX1) whereas, in contrast, the pro-apoptotic related genes (BAX, CASP3) were downregulated as shown in figure 10.

Discussion

Neurodegenerative diseases cause loss of neurons from different parts of the brain and unlike other cells, neuronal loss cannot be restored over time, causing permanent damage once its property is lost. SH-SY5Y cell lines are one of the most common neuroblastoma cell lines used for the *in vitro* studies for neuronal modelling[27]. The inability to reduce the overproduction of reactive oxygen species in the brain is considered as one of the major reasons for neurodegeneration and suppression of dopamine secretion in the substantia nigra[40]. Healthy SH-SY5Y cells exhibit a spindle shape with an elongated structure and an intact nucleus. Unlike healthy SH-SY5Y cells, stressed cells exhibit a shrinkage of the nucleus with a lesser spindle over the edges or even blunt edges with an oval-like structure[39,63].

The characterisation of SI-extract through TEM[46] evaluates the morphology as round and spherical in shape with an inner and outer shell-like structure. The peaks obtained from qualitative HPLC[49] show the presence of small phenolic compounds and shorter peptides at 6.196 and 6.499 minutes which overlap with each other. The peak at 7.601 minutes indicates the presence of polar pigment or a possibility for a larger peptide. At 8.785 minutes, melanin pigment is eluted towards the end, due to its larger molecular weight, which is represented by a broad peak, which resembles the richness of the compound.

To further investigate our marine sample, the half maximal inhibitory concentration (IC_{50}) was evaluated through cytotoxicity studies using 3-(4,5-dimethylthiazol-2-yl)-2,5-diphenyltetrazolium bromide (MTT) assay[66] where the IC_{50} values of SI extracts in control, hydrogen peroxide and acrylamide were 77±0.14, 79±0.17 and 82±0.21 µg/ml respectively. The viability of SH-SY5Y cells increased with an increase in concentration whereas in contrast, at higher concentrations, the cell viability reduced. Hence, these IC_{50} values were chosen for further evaluation of the extract.

Hydrogen peroxide (H_2O_2) is a powerful oxidant and acrylamide, at elevated concentrations, acts as a major factor for increased neuronal degeneration due to the oxidative stress induced in the SH-SY5Y cell line[8,10,48,68]. The intracellular ROS was quantified through fluorescence emission where the higher intensity of the fluorescence represents increased apoptosis of the cells whereas the lower fluorescence represents that the cell is viable[64]. The ROS assay was examined using DCFH-DA[6,75] where the cells with no treatment exhibited 79%, 83% and 89% SI extract showed 38%, 26% and 22% and LD treatment exhibited 57%, 43% and 38% in control, hydrogen peroxide and acrylamide-induced groups respectively. From this study, it is evident that the SI extract has significant antioxidant potential and the p-value was ($p < 0.05$) which is statistically significant.

In addition to this, the wound healing assay[21] exhibited wound closure in SI-treated of control, hydrogen peroxide and acrylamide induced groups with 88.5%, 80.45% and 87.45% and in LD-treated groups with a percentage wound healing of 78.85%, 68.75% and 72.35% respectively. The p-value was $p<0.05$ with a significant difference, providing insights that SI-extract promotes wound healing properties.

Further, the investigation on nuclear fragmentation through DAPI assay provides insights on the DNA fragmentation of the cells which was achieved through DAPI staining and visualization under fluorescence microscope[28]. The stress-induced cells upon treatment with SI-extract revealed uniform, round nuclei with moderate fluorescence in SI-treated cells indicating intact and healthy nucleus. The untreated stress-induced cells exhibited a condensed and

fragmented and shrunken nuclei and discrete apoptotic bodies. These changes in cell exhibit an elevated intracellular ROS[30]. The cells treated with SI-extract exhibited 17.55%, 56.45% and 53.33% in control, hydrogen peroxide and acrylamide groups respectively. From this study, we interpret that SI-treated cells have $p < 0.05$, which is significant with an intact and healthy cell morphology which signifies its potential neuroprotective effects.

In the present study, the potential of cell proliferation was evaluated using the standard method to determine the cell viability[60,61]. The stress-induced group showed a reduced proliferation compared to the control group, confirming the cytotoxic effects of oxidative stress in untreated cells. The cells pre-treated with the SI-extract exhibited an increase in proliferation. The SI-treated groups with H_2O_2 and acrylamide, demonstrated a statistically significant improvement in cell viability ($p < 0.05$) compared to the untreated groups. The LD-treated under the identical stress conditions showed proliferation for control, hydrogen peroxide and acrylamide as 78.85%, 76.75% and 82.15% respectively. In contrary, the LD-treated cells in control, hydrogen peroxide and acrylamide groups exhibited 59.45%, 57.65% and 54.34% respectively.

Similarly, the flow cytometry analysis reveals the apoptosis and cell viability[37] profiles which exhibited that the SI-treated groups protected the cells from apoptotic cell death in the control and stress-induced groups. The percentages of cell viability in SI-treated groups were 88.82% (control), 50.97% (H_2O_2) and 85.56% (acrylamide) treated groups. In contrast, in the LD-treated cells, the cell viability was evaluated as 47.62% (control), 40.83% (H_2O_2) and 42.26% (acrylamide) and the cells with no drug treated showed only 16.46% of viable cells. The p-value of the SI-treated groups ($p < 0.05$) was significant and exhibits neuroprotective effects.

Finally, the gene expression studies evaluated through RT-qPCR give us insights on the upregulation and downregulation of antioxidant and anti-apoptotic genes and the downregulation of pro-apoptotic genes[71] respectively in stress-induced and control cells. The upregulation of the antioxidant genes in control, hydrogen peroxide and acrylamide stress-induced cells in SOD1 was 3.0-, 2.7- and 1.5- fold increase. In CAT, it was 2.3-, 1.5- and 2.0- fold increase, 3.0-, 2.8- and 1.5- fold increase in GPX1 and 3.5-, 2.5- and 3.0- fold increase for GPX2 respectively. Similarly, the anti-apoptotic genes exhibited upregulation in the control, hydrogen peroxide and acrylamide cells where the fold change as calculated by $2^{-\Delta\Delta Ct}$ method in BCL-2 was 2.9-, 2.0- and 2.5- fold increase, 3.1-, 2.5- and 3.0- fold change for BCL-XL respectively indicating that the increase in fold change prevents the cells from cell death or apoptosis and thereby increases the cell viability.

In contrast to this, the downregulation of pro-apoptotic genes in control, hydrogen peroxide and acrylamide stress-induced cells in BAX was 2.0-, 0.6- and 1.8- fold decrease and 1.9-, 1.4- and 1.6- fold decrease for CASP2 respectively. From our findings, we suggest that the upregulation of antioxidant and anti-apoptotic genes prevents the cells from oxidants and preserves the cells from damage, ultimately leading to apoptosis, which tends to neuronal loss. This suggests that the SI-derived bioactive extract exerts a neuroprotective potential through mitigating ROS-induced cell damage through antioxidant mechanisms and wound healing properties.

Conclusion

Oxidative stress is a major factor in inducing neurodegeneration in the substantia nigra, which further leads to dopamine suppression over a longer period of time, causing PD. Marine sources have been extensively used in potential new drug discovery for treating neurodegenerative diseases. Levodopa combined with carbidopa is the standard drug treatment for PD. Even so, to overcome the shortcomings of the stability and prolonged exposure to a single drug effect, potential compounds are discovered to increase the quality of treatment in neurodegenerative diseases. SI-extract has shown a significant difference in the stress-induced models by downregulating the pro-apoptotic genes and upregulating the antioxidant and anti-apoptotic genes, which symbolize the potential for neuroprotective properties.

Additionally, the evaluation of flow cytometry exhibited increased cell viability in SI-treated cells. Moreover, the ROS assay showed less fluorescence in comparison to the control and standard groups, confirming that the SI-treated cells have potential antioxidant activity. Overall, the SI extract shows potential antioxidant activities and it can be further analysed and tested for its clinical importance in drug discovery from marine sources of neurodegenerative diseases to overcome the shortcomings of existing drug treatment.

Acknowledgement

The authors would like to express their sincere gratitude to Vellore Institute of Technology, Vellore, for providing support to pursue this research.

References

1. Aldred J. et al, Efficacy and Safety of Foslevodopa/ Foscarbidopa Monotherapy in Patients with Parkinson's Disease, *Mov Disord Clin Pract.*, doi: 10.1002/mdc3.70245 **(2025)**

2. Ali R. et al, Hydrogen Sulfide-Releasing Insulin Polypeptide Mitigates Hyperglycemia-Induced Neurotoxicity and Cognitive Deficits *In Vivo*, *ACS Chem Neurosci.*, **16(17)**, 3323-39 **(2025)**

3. Altin-Celik P., Derya-Andeden M., Eciroglu-Sarban H. and Donmez-Altuntas H., Antiproliferative and apoptotic effects of Pervari honey on SH-SY5Y neuroblastoma cells, *Med Oncol.*, **42(9)**, 394 **(2025)**

4. Ashok C. et al, Comparative evaluation of MPTP and rotenone

as inducing agents for Parkinson's disease in adult zebrafish: Behavioural and histopathological insights, *Toxicol Reports*, **15**, 102084 **(2025)**

5. Barangi S., Hosseinzadeh P., Karimi G., Tayarani Najaran Z. and Mehri S., Osthole attenuated cytotoxicity induced by 6-OHDA in SH-SY5Y cells through inhibition of JAK/STAT and MAPK pathways, *Iran J Basic Med Sci*., **26(8)**, 953–9 **(2023)**

6. Bhargavi Lakshmi J., Bhaskar Pittala, Laxminarayana Eppakayala, Paramesh Donta and Chittireddy Venkata Ramana Reddy, In silico and antibacterial studies of Thiadiazole and Triazole linked 1,8-Napthyridine derivatives, **29(1)**, *Res. J. Chem. Environ*., 46-51 **(2025)**

7. Bridgeman L., Juan C., Berrada H. and Juan-García A., Effect of Acrylamide and Mycotoxins in SH-SY5Y Cells: A Review, *Toxins (Basel)*, **16(2)**, 87 **(2024)**

8. Bridgeman L., Juan C., Berrada H. and Juan-García A., Investigating the effect of acrylamide, penitrem A and 3-acetyldeoxynivalenol in SH-SY5Y human neuroblastoma cells: exploring the oxidative stress, *Toxicon*, **264**, 108441 **(2025)**

9. Cha H.R., Kim J.S., Ryu J.H. and Cho H.J., Investigating Neuroprotective Effects of Berberine on Mitochondrial Dysfunction and Autophagy Impairment in Parkinson's Disease, *Int J Mol Sci.*, **26(15)**, 7342 **(2025)**

10. Chen W.T. et al, Thermal cycling protects SH-SY5Y cells against hydrogen peroxide and β-amyloid-induced cell injury through stress response mechanisms involving Akt pathway, *PLoS One*, **15(10)**, e0240022 **(2020)**

11. Cheung S. et al, Mechanism interpretation of Guhan Yangshengjing for protection against Alzheimer's disease by network pharmacology and molecular docking, *J Ethnopharmacol*., **328**, 117976 **(2024)**

12. Chib S., Singh S., Singh R. and Amanat M., Manganese overexposure: Unveiling its neurotoxic potential and involvement in pathogenesis of Parkinson's disease, *J Trace Elem Med Biol Organ Soc Miner Trace Elem*., **91**, 127721 **(2025)**

13. Choi S.B., Kwon S., Kim J.H., Ahn N.H., Lee J.H. and Yang S.H., The Molecular Mechanisms of Neuroinflammation in Alzheimer's Disease, the Consequence of Neural Cell Death, *Int J Mol Sci*., **24(14)**, 11757 **(2023)**

14. Elangovan S. and Arumugam S., Purification, characterization and biological activities of melanin pigment isolated from Indian squid Uroteuthis duvaucelii, *Aquac Int.*, **31(6)**, 3095–108 **(2023)**

15. Fang J., Kuwamoto W., Miranda G., Rajagopalan V. and Elul T., Quantifying Morphology of a Differentiating Neuroblastoma Cell Line, *MicroPublication Biol.*, doi: 10.17912/micropub.biology.001099 **(2024)**

16. Fatima S.J. and Prasad D.K., Enhanced Neuroprotection by Diosgenin and Pterostilbene Combination Against Neurotoxicity Induced by Amyloid-B 1-42 in SH-SY5Y Differentiated Cell Models, *Ann Neurosci*., doi: 10.1177/09727531251356049 **(2025)**

17. Feles S. et al, Streamlining Culture Conditions for the Neuroblastoma Cell Line SH-SY5Y : A Prerequisite for Functional Studies, *Methods Protoc.*, **5(4)**, 58 **(2022)**

18. Gadhave D.G. et al, Neurodegenerative disorders: Mechanisms of degeneration and therapeutic approaches with their clinical relevance, *Ageing Res Rev*., **99**, 102357 **(2024)**

19. Griesshaber E. et al, Biological light-weight materials: The endoskeletons of cephalopod mollusks, *J Struct Biol*., **215(3)**, 107988 **(2023)**

20. Guatteo E., Berretta N., Monda V., Ledonne A. and Mercuri N.B., Pathophysiological Features of Nigral Dopaminergic Neurons in Animal Models of Parkinson's Disease, *Int J Mol Sci*., **23(9)**, 4508 **(2022)**

21. Huang N. et al, Preparation and evaluation of squid ink polysaccharide-chitosan as a wound-healing sponge, *Mater Sci Eng C.*, **82(1)**, 354–62 **(2018)**

22. Huang Y. et al, MicroRNA-9-5p Alleviates Oxidative Stress, Inflammation and Apoptosis in Cerebral Ischemia-reperfusion Injury by Targeting NOX4 *In vitro*, *Curr Mol Med.*, doi: 10.2174/0115665240337045241210064142 **(2025)**

23. Hussain M.S., Ramalingam P.S. and Bisht A.S., Stem Cell Nanotechnology Applications as Drug Delivery Systems for Neurodegenerative Disorders, Current pharmaceutical design, United Arab Emirates, 2148–50 **(2025)**

24. Hussain M.S. et al, Unveiling polyphyllin's role in neuroprotection: A pharmacological perspective, *Pharmacol Res - Mod Chinese Med*., **16,** 100641 **(2025)**

25. Islam M.R. et al, Clinical and Mechanistic Exploration of Ellagic Acid in Neurodegenerative Diseases: Targeted Neuroprotection Through Cellular and Molecular Mechanisms, *Chem Biodivers*, **22(10),** e00105 **(2025)**

26. Izumi Y., Kondo N., Akaike A., Koyama Y. and Kume T., Perilla-derived chalcone inhibits α-synuclein fibrillization and prevents aggregate-induced disruption of intracellular α-synuclein conformation in neuronal cells, *Biochem Biophys Res Commun*., **779**, 152452 **(2025)**

27. Jiang Y. et al, Protective Effects of Querectin against MPP(+)-Induced Dopaminergic Neurons Injury via the Nrf2 Signaling Pathway, *Front Biosci*, **28(3)**, 42 **(2023)**

28. Jung Y.J., Choi H. and Oh E., Melatonin attenuates MPP(+)-induced apoptosis via heat shock protein in a Parkinson's disease model, *Biochem Biophys Res Commun*., **621**, 59–66 **(2022)**

29. Kara M. et al, *In vitro* mechanistic studies and potential health benefits of a standardized bilberry extract in low mood and cognitive enhancement, *Front Nutr*., **12**, 1630147 **(2025)**

30. Karavelioglu Z. and Cakir-Koc R., Preparation of chitosan nanoparticles as Ginkgo Biloba extract carrier: *In vitro* neuroprotective effect on oxidative stress-induced human neuroblastoma cells (SH-SY5Y), *Int J Biol Macromol*., **192**, 675–83 **(2021)**

31. Kaur S. et al, Alpha-asarone protects against rotenone-induced

neurotoxicity in a rat model of Parkinson's disease, *Neurol Res*., **47(11),** 1084-1103 **(2025)**

32. Kocanci F.G., Effect of Pimecrolimus on apoptotic pathways in H(2)O(2)-treated neuron like differentiated-SH-SY5Y cells: a molecular docking and mechanistic study, *Toxicol Res (Camb)*, **14(1)**, tfaf020 **(2025)**

33. Krunić M. et al, Graphene quantum dot antioxidant and proautophagic actions protect SH-SY5Y neuroblastoma cells from oxidative stress-mediated apoptotic death, *Free Radic Biol Med*., **177**, 167–80 **(2021)**

34. Kumar J., Varela-Ramirez A. and Narayan M., Development of novel carbon-based biomedical platforms for intervention in xenotoxicant-induced Parkinson's disease onset, *BMEmat*, **2(4)**, e12072 **(2024)**

35. Kumar N., Halcrow P.W., Quansah D.N.K., Liang B., Meucci O. and Geiger J.D., Involvement of endolysosome iron in HIV-1 gp120-, morphine- and iron supplementation-induced disruption of the reactive species interactome and induction of neurotoxicity, *Redox Rep.*, **30(1)**, 2546496 **(2025)**

36. Lee T.Y. et al, 5-HT(7) antagonists confer analgesia via suppression of neurotrophin overproduction in submucosal nerves of mouse models with visceral hypersensitivity, *J Physiol*., **603(17),** 4723-4745 **(2025)**

37. Lee Y.Y. et al, Standardization of Germinated Oat Extracts and Their Neuroprotective Effects Against Aβ(1-42) Induced Cytotoxicity in SH-SY5Y Cells, *Molecules*, **30(15)**, 3291 **(2025)**

38. Li G. et al, N-butylphthalide (NBP) and ligustrazine (TMP) triazole hybrids target the KEAP1-NRF2 pathway to inhibit ferroptosis and exert brain neuroprotectivity, *Redox Biol*., **86**, 103835 **(2025)**

39. Li Y. et al, Overexpression of methionine sulfoxide reductase A alleviates acrylamide-induced neurotoxicity by mitigating lipid peroxidation and mitochondria-dependent apoptosis *In vivo* and *In vitro*, *Food Chem Toxicol an Int J Publ Br Ind Biol Res Assoc*., **199**, 115339 **(2025)**

40. Liu T., Kong X., Qiao J. and Wei J., Decoding Parkinson's Disease: The interplay of cell death pathways, oxidative stress and therapeutic innovations, *Redox Biol.*, **85**, 103787 **(2025)**

41. Luo Q., Hu W., Yu H., Zhang R. and Chen X., 11,12-Diacetyl-carnosol Protects SH-SY5Y Cells from Hydrogen Peroxide Damage through the Nrf2/HO-1 Pathway, *Evid Based Complement Alternat Med*., **2022**, 4376812 **(2022)**

42. Mallardo M., Nigro E., Bianco C., Defez R., Valenti A. and Daniele A., Insights from an in vitro study: the anti-proliferative effects of indole-3-acetic acid in neuroblastoma cells, *Biochem Pharmacol*., **242**, 117231 **(2025)**

43. Miyaue N. and Nagai M., Sex differences in the pharmacokinetics of levodopa and carbidopa in patients with Parkinson's disease, *Parkinsonism Relat Disord*, **139**, 108006 **(2025)**

44. Moura C., Gouveia M.J. and Vale N., Repurposed Antipsychotics as Potential Anticancer Agents: Clozapine Efficacy and Dopaminergic Pathways in Neuroblastoma and Glioblastoma, *Life* (Basel, Switzerland), **15(7)**, 1097 **(2025)**

45. Negishi T. et al, Diphenylarsinic acid induced astrocyte-preferential cell-type-specific aberrant activation of signal transduction related to oxidative stress, MAP kinase activation, transcription factor regulation and glutathione metabolism, *J Toxicol Sci*., **50(6)**, 293–308 **(2025)**

46. Niyonkuru D. et al, A nanoscale study of the structure and electrical response of Sepia eumelanin, *Nanoscale Adv*., **5(19)**, 5295–300 **(2023)**

47. Norota I. et al, Midnolin gene expression is enhanced by G(q)-coupled muscarinic acetylcholine receptor stimulation in SH-SY5Y human neuroblastoma cells, *J Pharmacol Sci*., **157(4)**, 229–32 **(2025)**

48. Pang Y., Chen J., Yang J., Xue Y., Gao H. and Gao Q., Protective effect and mechanism of Lycium ruthenicum polyphenols against acrylamide-induced neurotoxicity, *Food Funct*., **14(10)**, 4552–68 **(2023)**

49. Panzella L. et al, Identification of black sturgeon caviar pigment as eumelanin, *Food Chem*., **373**, 131474 **(2022)**

50. Perlikowska R., Długosz-Pokorska A., Domowicz M., Grabowicz S., Stasiołek M. and Zakłos-Szyda M., Reduction in SH-SY5Y Cell Stress Induced by Corticosterone and Attenuation of the Inflammatory Response in RAW 264.7 Cells Using Endomorphin Analogs, *Biomedicines*, **13(7)**, 1774 **(2025)**

51. Pluta R., Kocki J., Kocka A.B., Bogucki J. and Czuczwar S.J., Alterations of Mitophagy (BNIP3), Apoptosis (CASP3) and Autophagy (BECN1) Genes in the Frontal Cortex in an Ischemic Model of Alzheimer's Disease with Long-Term Survival, *Curr Alzheimer Res*., **22(6)**, 442-455 **(2025)**

52. Que R. et al, Dl-3-n-Butylphthalide Rescues Dopaminergic Neurons in Parkinson's Disease Models by Inhibiting the NLRP3 Inflammasome and Ameliorating Mitochondrial Impairment, *Front Immunol*., **12**, 794770 **(2021)**

53. Rademacher K. et al, Chronic hyperactivation of midbrain dopamine neurons causes preferential dopamine neuron degeneration, *Elife*, Preprint, 13 **(2025)**

54. Ramalingam P.S. et al, Synergistic anticancer effects of camptothecin and sotorasib in KRAS -mutated pancreatic ductal adenocarcinoma, *Frontiers in Pharmacology*, **16**, 1–21 **(2025)**

55. Rehfeldt S.C.H., Laufer S. and Goettert M.I., A Highly Selective *In Vitro* JNK3 Inhibitor, FMU200, Restores Mitochondrial Membrane Potential and Reduces Oxidative Stress and Apoptosis in SH-SY5Y Cells, *Int J Mol Sci.*, **22(7)**, 3701 **(2021)**

56. Rehfeldt S.C.H. et al, Neuroprotective Effect of Luteolin-7-O-Glucoside against 6-OHDA-Induced Damage in Undifferentiated and RA-Differentiated SH-SY5Y Cells, *Int J Mol Sci*., **23(6)**, 2914 **(2022)**

57. Safari M., Yousefi M., Jenkins H.A., Torbati M.B. and

Amanzadeh A., Synthesis, spectroscopic characterization, X-ray structure and *in vitro* antitumor activities of new triorganotin(IV) complexes with sulfur donor ligand, *Med Chem Res*., **22(12)**, 5730–8 **(2023)**

58. Sannino A., Allocca M., Scarfì M.R., Romeo S. and Zeni O., Protective effect of radiofrequency exposure against menadione-induced oxidative DNA damage in human neuroblastoma cells: The role of exposure duration and investigation on key molecular targets, *Bioelectromagnetics*, **45(8)**, 365–74 **(2024)**

59. Shandilya C. and Mani S., Rho kinase isoforms in neurodegeneration: from cellular functions to therapeutic targets, *Mol Biol Rep.*, **52(1)**, 846 **(2025)**

60. Summart R., Imsoonthornruksa S., Yongsawatdigul J., Ketudat-Cairns M. and Udomsil N., Characterization and molecular docking of tetrapeptides with cellular antioxidant and ACE inhibitory properties from cricket (Acheta domesticus) protein hydrolysate, *Heliyon*, **10(15)**, e35156 **(2024)**

61. Tidke B. et al, Therapeutic Implications of Allopregnanolone in Alzheimer's Related Depression, *Behav Brain Res*., **495**, 115785 **(2025)**

62. Treccani S. et al, Poly-L-lactic acid nanofiber/polyamidoamine composite hydrogel as novel strategy for *in vitro* neuroregeneration and neuroprotection, *Biomater Adv*., **177**, 214415 **(2025)**

63. Vulin I., Tenji D., Teodorovic I. and Kaisarevic S., Undifferentiated versus retinoic acid-differentiated SH-SY5Y cells in investigation of markers of neural function in toxicological research, *Toxicol Mech Methods*, **35(1)**, 53–63 **(2025)**

64. Wang Y., Bai G., Mu S., Zhang F. and Wang Y., Indobufen alleviates ischemic stroke injury by regulating transcription factor NRF2 and inhibiting ATG5 expression, *J Pharm Pharmacol*., **76(7)**, 842–50 **(2024)**

65. Wu L.K. et al, Artemisia Leaf Extract protects against neuron toxicity by TRPML1 activation and promoting autophagy/ mitophagy clearance in both *in vitro* and *in vivo* models of MPP+/MPTP-induced Parkinson's disease, *Phytomedicine*, **104**, 154250 **(2020)**

66. Xie W. et al, Notoginseng Leaf Triterpenes Ameliorates OGD/R-Induced Neuronal Injury via SIRT1/2/3-Foxo3a-MnSOD /PGC-1α Signaling Pathways Mediated by the NAMPT-NAD Pathway, *Oxid Med Cell Longev.*, **2020**, 7308386 **(2020)**

67. Xu Q., Xie D., Qie X., Chi B. and Liu H., Effect of Self-Assembled Polydopamine Nanoparticles on Ferroptosis in an MPTP-Induced Parkinson's Disease Mice Model, *ACS Appl Bio Mater*., **8(8)**, 7410–9 **(2025)**

68. Yıldız F., Investigation of neuroprotective effects of newly synthesized benzimidazolium salt against neurotoxicity in differentiated SH-SY5Y neuronal cells, *Biochem Biophys Res Commun.*, **777**, 152255 **(2025)**

69. Yu X., Cai H., He C., Ouyang Z., Li Y. and Chen L., Regulatory role of LncRNA FMR1-AS1 in the pathogenesis of alzheimer's disease based on bioinformatics and *in vitro* experimental validation, *Sci Rep.*, **15(1)**, 30134 **(2025)**

70. Zeng W., Wang Y., Liu Y., Liu X. and Qi Z., Garlic-Derived Allicin Attenuates Parkinson's Disease via PKA/p-CREB/BDNF/ DAT Pathway Activation and Apoptotic Inhibition, *Molecules*, **30(15)**, 3265 **(2025)**

71. Zhai C.Y., Fan J.S. and Zhang R.P., Scutellarein treats neuroblastoma by regulating the expression of multiple targets, *Ibrain*, **10(3)**, 345–55 **(2024)**

72. Zhang J. et al, Tamibarotene promotes differentiation of neuroblastoma SH-SY5Y cells into neurons, which is associated with activation of the PI3K/AKT signaling pathway, *BMC Neurosci.*, **26(1)**, 41 **(2025)**

73. Zhao M., Zhang B., Deng L. and Zhao L., Acrylamide Induces Neurotoxicity in SH-SY5Y Cells via NLRP3-mediated Pyroptosis, *Mol Neurobiol.*, **60(2)**, 596–609 **(2023)**

74. Zhao Z. et al, ECHS1-NOX4 interaction suppresses rotenone-induced dopaminergic neurotoxicity through inhibition of mitochondrial ROS production, *Free Radic Biol Med.*, **232**, 56–71 **(2025)**

75. Zheng T., Zheng C., Gao F., Huang F., Hu B. and Zheng X., Dexmedetomidine suppresses bupivacaine-induced parthanatos in human SH-SY5Y cells via the miR-7-5p/PARP1 axis-mediated ROS, *Naunyn Schmiedebergs Arch Pharmacol.*, **394(4)**, 783–96 **(2021)**.

(Received 04th September 2025, accepted 06th October 2025)